Available online at www.sciencedirect.com
SCIENCE DIRECT®
Journal of Organometallic Chemistry 691 (2006) 3189–3195
Journal of Organometallic Chemistry
www.elsevier.com/locate/jorganchem

Syntheses and characterizations of methylpalladium complexes bearing a biphenyl-based bulky phosphine ligand: Weak interactions suggested by NBO and QTAIM analyses

Makoto Yamashita, Ikuko Takamiya, Koichiro Jin, Kyoko Nozaki *

Department of Chemistry and Biochemistry, Graduate School of Engineering, The University of Tokyo, 7-3-1 Hongo, Bunkyo-ku, Tokyo 113-8656, Japan

Received 19 January 2006; received in revised form 2 February 2006; accepted 2 February 2006
Available online 10 March 2006

Abstract

A methylpalladium chloride complex bearing a biphenyl-based bulky phosphine ligand, ^{t}Bu$_2$P(biphenyl-2-yl) (**1**), namely [Pd(**1**)(Me)Cl]$_2$ (=**8**), was synthesized by the reaction of (cod)Pd(Me)Cl with **1**. A following reaction of **8** with AgOTf gave the corresponding triflate complex, Pd(**1**)(Me)OTf (=**9**). These complexes were fully characterized by NMR spectroscopy and structurally characterized by X-ray crystallographic study. In the solid state of **8**, biphenyl-based phosphine ligand **1** played a role of monodentate phosphine ligand with a possible weak η^1-coordination from the phenyl ring at 2′-position of **1**. On the other hand, phosphine ligand **1** in **9** showed a bidentate coordination mode consist of σ-donation of the phosphine and η^2-coordination of the phenyl ring at 1′- and 2′-positions. Natural bond orbital (NBO) and quantum theory of atoms in molecules (QTAIM) calculations also supported the existence of these weak interactions.

Keywords: Bulky phosphine ligand; Alkylpalladium complex; Hapticity; Wiberg bond indices; Atoms in molecules

1. Introduction

Over the past few years, biphenyl- or binaphthyl-based monophosphines are widely known as ligands in various palladium-catalyzed reactions [1–24]. Buchwald reported many biphenyl-based phosphine ligands for cross-coupling reactions (**1**–**5** in Fig. 1) [1–17]. On the other hand, Hayashi reported binaphthyl-based monodentate phosphine ligands (MOP (**6**) [18–23] to achieve highly efficient asymmetric hydrosilylation and allylic substitution reactions. Vyskočyl, Kočovský, Ding, and Mikami also reported a derivatization of MOP to MAP (**7**) and its application to the asymmetric allylic substitution [25,26]. Extensive studies about these catalyst systems were reported to disclose the origin of unique properties of the biphenyl- or binaphthyl-based ligands. These studies include the isolation of Pd(0) complexes as intermediates for the cross-coupling reaction and the isolation of allylpalladium(II) complexes as intermediates for the allylic substitution reaction [7,13,17,20,21,27–34]. Some of them showed the specific coordination mode of the biphenyl-based ligands, i.e., η^1- [13,27–29,32] or η^2-coordination [7,27,30,31] of arene ring to the central palladium atom. The nature of the bindings were carefully studied by Pregosin et al. [28,31,35] and Faller and Sarantopoulos [30] using NMR spectroscopy. Herein, we report syntheses of two methylpalladium complexes **8** and **9** bearing a biphenyl-based ligand. These are the first examples of alkylpalladium complexes bearing a biarylphosphine ligand. A coordination mode change of the biphenyl-based ligand from η^1 to η^2 by changing the anionic ligand on the palladium from Cl to OTf was observed. Furthermore, NBO and QTAIM analyses were performed to evaluate the relative strength of these weak coordinations.

---

* Corresponding author. Tel./fax: +81 3 5841 7261.
E-mail address: nozaki@chembio.t.u-tokyo.ac.jp (K. Nozaki).

0022-328X/$ - see front matter © 2006 Elsevier B.V. All rights reserved.
doi:10.1016/j.jorganchem.2006.02.001

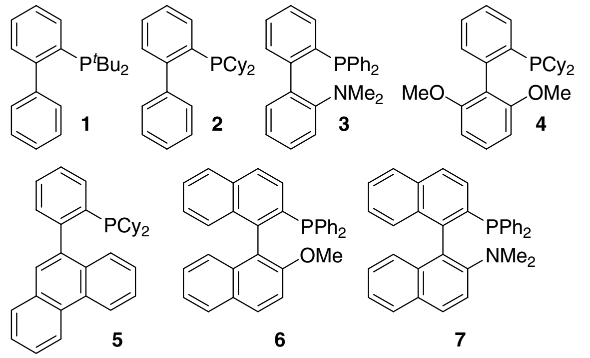

Fig. 1. Biphenyl- or binaphthyl-based phosphine ligands.

2. Results and Discussion

A simple ligand exchange reaction of (cod)Pd(Me)Cl [36,37] with **1** [3,38,39] afforded the corresponding monophosphine-ligated methylpalladium chloride complex **8** as a crystalline yellow solid in 90% yield (Scheme 1). Chloride abstraction of **8** by silver triflate gave a methylpalladium triflate complex **9** in 71% yield.

In solution, these two complexes showed essentially similar NMR spectra for ^{1}H and ^{13}C nuclei. In the ^{1}H NMR spectra, both **8** and **9** showed seven kinds of sharp signals in aromatic region (two of them were seemed to be overlapped), where the D_2 symmetry of the terminal phenyl ring indicated the free rotation of the phenyl ring in NMR time scale. In the ^{13}C NMR spectra, 10 kinds of sharp aromatic signals were observed for both **8** and **9**, also indicating the free rotation of the terminal phenyl ring similar to that of the free ligand **1** [38,40].

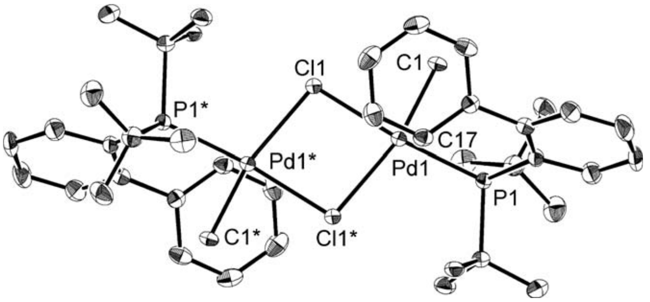

Fig. 2. ORTEP drawing of **8** (all hydrogen atoms are omitted for clarity).

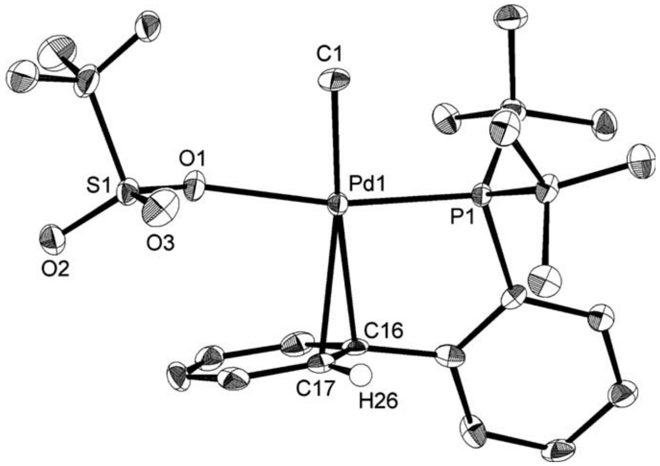

Fig. 3. ORTEP drawing of **9** (all hydrogen atoms except H26 are omitted for clarity).

Table 1
Selected bond distances (Å) and bond angles (°) for complexes **8** and **9**

	8	9
Pd(1)–C(1)	2.037(4)	2.042(6)
Pd(1)–P(1)	2.2644(11)	2.2368(19)
Pd(1)–Cl(1)	2.4019(11)	
Pd(1)–Cl(1*)	2.4645(12)	
Pd(1)–O(1)		2.214(4)
Pd(1)–C(16)	3.297(4)	2.538(5)
Pd(1)–C(17)	2.955(4)	2.507(6)
C(1)–Pd(1)–Cl(1)	85.11(11)	
C(1)–Pd(1)–P(1)	88.57(12)	
P(1)–Pd(1)–Cl(1)	171.70(4)	
C(1)–Pd(1)–O(1)		81.51(19)
C(1)–Pd(1)–P(1)		90.31(17)
P(1)–Pd(1)–O(1)		167.43(11)

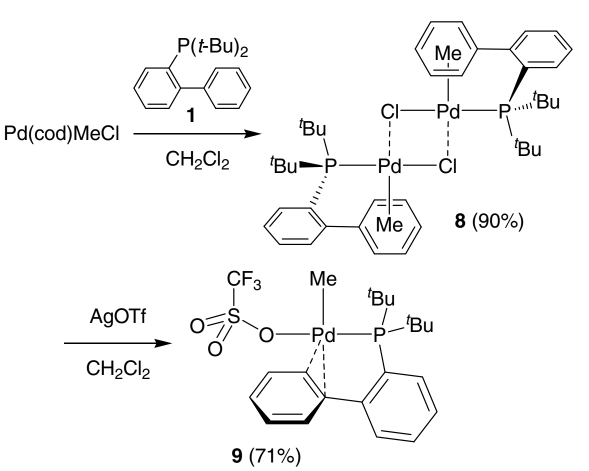

Scheme 1. Syntheses of methylpalladium chloride complex **8** and triflate complex **9**.

Both **8** and **9** were structurally characterized by X-ray crystallography. The solid state structures of them are shown in Figs. 2 and 3. Selected bond lengths and bond angles are shown in Table 1. The X-ray crystallographic analysis revealed that **8** has a Cl-bridged dinuclear structure where a half of the dinuclear structure is an asymmetric unit. In spite of the bulkiness of the ligands, bond lengths and angles around the central palladium atom in **8** are similar to those of previous Cl-bridged dinuclear complexes bearing a common triarylphosphine [41–44]. There is only one reported example of a neutral organopalladium(II) chloride complex, Pd(**6**)(allyl)Cl, bearing a biaryl-based phosphine ligand [20]. The structure of methylpalladium complex **8** is different from that of Pd(**6**)(allyl)Cl, where the palladium has a mononuclear square planar structure consist of a phosphorus atom, a chlorine atom, and η^3-allyl group [20].

In contrast to **8**, one of phenyl rings of biphenyl moiety in **9** coordinated to the palladium center as a neutral η^2-

ligand to form square planar palladium (Pd(1)–C(16) = 2.538(5) Å, Pd(1)–C(17) = 2.507(6) Å). This type of η^2-coordination mode has been observed in the neutral palladium(0) [7] or cationic palladium(II) [27,30,31] complexes bearing a biphenyl- or binaphthyl-based ligand. Relatively long Pd–C distances in **9** and no lower-field shift of ^{13}C NMR peaks for the coordinating carbon atoms showed the η^2-coordination is weaker than the previously reported examples [7,27,30,31] probably due to the strong *trans* influence of methyl group.

The difference of the solid-state structures between **8** and **9** may come from the electron density of the central palladium atom and the bridging ability of the anionic ligands. In the case of **8**, the coordination of bridging chloride may be stronger than η^2-coordination of phenyl ring. In the case of **9**, electron density of the palladium was lowered by triflate anion, so the η^2-coordination of phenyl ring may be stronger than that of bridging triflate.

Although the solid-state structures of **8** and **9** were different, the solution state structures of them are proposed to be similar due to the following reasons. The rotations of the terminal phenyl ring of **1** in both **8** and **9** are very fast as was suggested that all the peaks of aromatic protons in ^{1}H NMR spectra of **8** and **9** kept their sharpness and D_2 symmetry in CD_2Cl_2 solution down to −80 °C. In the case of **9**, the free rotation of the phenyl ring can be considered to take place through a cleavage of η^2-coordination to form a formal three-coordinate palladium complex **9A** as illustrated in Scheme 2. One can also expect that there is an equilibrium in the solution of **8** to form the corresponding mononuclear complex Pd(**1**)(Me)Cl (=**8A**). This assumption is supported by a reported equilibrium between dinuclear and mononuclear complexes in [(*o*-tol)$_3$PPd(*p*-tol)Br]$_2$ [45].

In solid state, a weak η^1-interaction between Pd(1) and C(17) in **8** may be suggested as fifth coordination as described in Fig. 4 [46]. The Pd(1)–C(17) distance (2.955(4) Å), which is the shortest distance among those between Pd and carbon atoms of the terminal phenyl ring, is shorter than the sum of van der Waals radii (3.30 Å) [47]. The η^1-coordination from the *ortho* carbon of biaryl moiety in **8** can be distinguished from the η^1-coordination from the ipso carbon of biaryl in the previously reported palladium complexes bearing a biaryl-phosphine ligand (Fig. 5, **10**–**12**) [13,27–29]. A similar η^1-coordination mode of biphenyl-based ligand from *ortho* carbon to the palladium was observed in a zerovalent palladium complex **13** [32]. A significant distortion of *ipso* carbon by X-ray was observed in **10**–**12**, in contrast, no such distortion of *ortho* carbon in **8** or **13** was observed. The possible η^1-coordination in **8** from *ortho* carbon of ligand **1** to the palladium should be even weaker than that in **13** [32] because the Pd(1)–C(17) distance (2.955(4) Å) is longer than that of **13** (2.676(5) Å). The relative weakness of Pd–C interaction in **8** is also estimated from the dynamic behavior in solution. The ^{1}H NMR peaks of **8** kept its symmetry down to −80 °C as described above although a broad ^{31}P NMR peak of **13** recoalesced into two peaks at −90 °C, indicating the rotation of the terminal phenyl ring in **8** is faster than an exchange of coordinating biaryl ring in **13** (see Table 2).

To evaluate the weak interactions between Pd(1) and C(17) in **8** and among Pd(1), C(16), and C(17) in **9**, Wiberg bond indices (WBI) [48] using natural bond orbital (NBO) and quantum theory of atoms in molecules (QTAIM) [49,50] analyses were performed at the X-ray structure (B3LYP/TZVPalls2/6-31G* for WBI, B3LYP/LANL2DZ/6-31G* for AIM). All the calculations were performed using GAUSSIAN 03 [51] and AIM2000 [52,53]. Wiberg bond indices and topological properties at bond

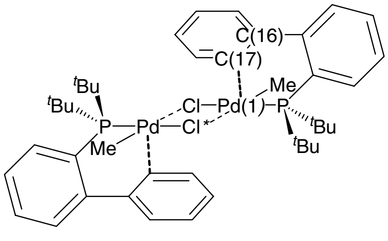

Fig. 4. Suggested weak η^1-coordination in **8** (dotted lines).

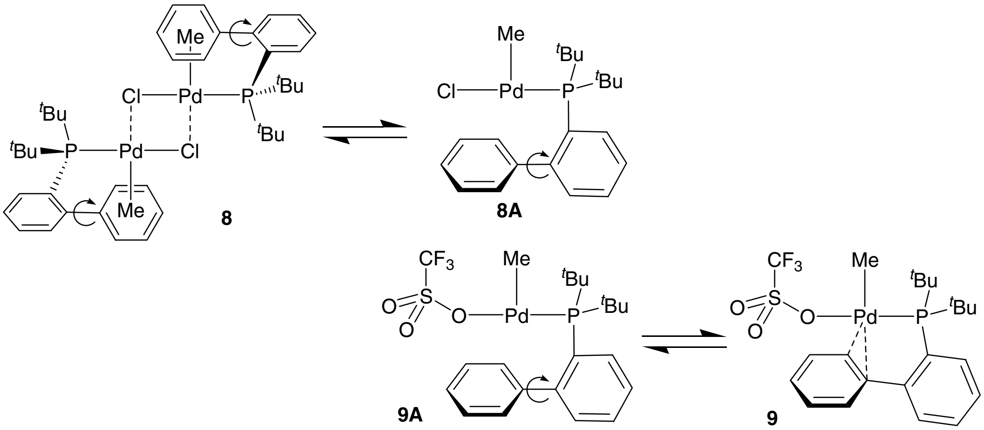

Scheme 2. Proposed equilibriums for **8** and **9** in solution.

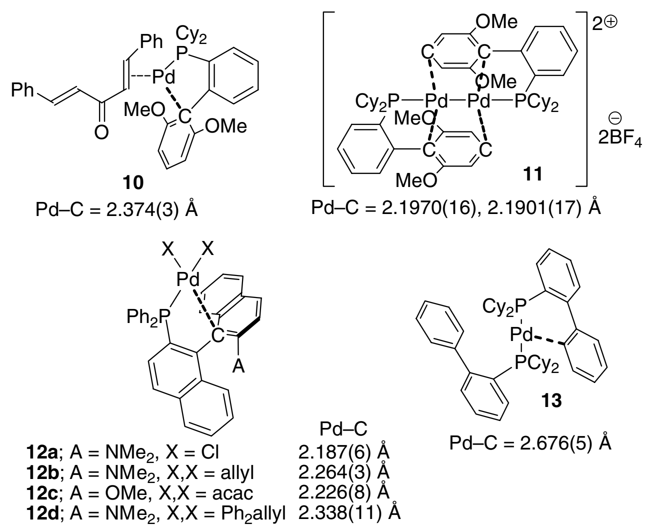

Fig. 5. Previously reported η^1-coordination in palladium complexes bearing a biaryl-based phosphine ligand and their Pd–C distances. Dotted lines describe the interaction between carbon and palladium.

Table 3
Interatomic distances (X-ray), Wiberg bond indices (WBI), and bond critical point properties (AIM) in **8** and **9** [58]

	Atoms	Distance (Å)	WBI	$\rho(\mathbf{r})$ (e/a_0^3)	$\nabla^2\rho(\mathbf{r})$ (e/a_0^5)
8	Pd(1)–C(17)	2.955(4)	0.0160	0.01778	0.05381
	Pd(1)–C(1)	2.037(4)	0.6252	0.12404	0.07505
	Pd(1)–P(1)	2.2644(11)	0.4751	0.09983	0.11798
	Pd(1)–Cl(1)	2.4019(11)	0.2325	0.06353	0.22930
	Pd(1)–Cl(1*)	2.4645(12)	0.1790	0.05563	0.20814
9	Pd(1)–C(16)	2.538(5)	0.0664	0.03822	0.13804
	Pd(1)–C(17)	2.507(6)	0.0712	0.03994	0.12704
	Pd(1)–C(1)	2.042(6)	0.6610	0.12010	0.06524
	Pd(1)–P(1)	2.2368(19)	0.5162	0.09061	0.11052
	Pd(1)–O(1)	2.214(4)	0.1519	0.06216	0.32360

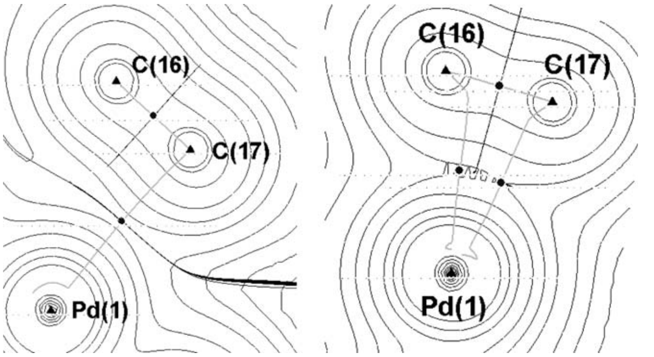

Fig. 6. Contour diagrams of $\rho(\mathbf{r})$ in **8** (left) and **9** (right). The triangles are (3, −3) critical points, which represent the location of nuclei. The solid circles are (3, −1) critical points, which are "bond critical point (BCP)". The lines connected two nucleus are bond paths, which describe interatomic interactions. Contour values: 0.001, 0.002, 0.004, 0.008, 0.02, 0.04, 0.08, 0.2, 0.4 and 0.8.

critical points (BCPs) in AIM for present study on **8** and **9** are summarized with interatomic distances in Table 3. Contour diagrams of $\rho(\mathbf{r})$ for the weak interactions in **8** and **9** are described in Fig. 6.

WBI value of 0.0160 for Pd(1)–C(17) in **8** was comparable to the reported WBI values of C–H agostic interactions between C–H bond of ^{t}Bu group and palladium in (^{t}Bu$_3$P)PdPhX (X = Br, I) (0.016, 0.015) [54] and between C–H bond of SiMe$_3$ group and yttrium in Y(NH$_2$)$_2$(NHSiMe$_3$) (0.013) [55]. Thus, η^1-coordination in **8** apparently exists although it is very weak. While, WBI values of 0.0664 for Pd(1)–C(16) and 0.0712 for Pd(1)–C(17) in **9** were larger than that of Pd(1)–C(17) in **8**.

Table 2
Crystallographic data and structure refinement details for **8** and **9**

	8	**9**
Formula	$C_{42}H_{60}Cl_2P_2Pd_2$	$C_{22}H_{30}F_3O_3PPdS$
FW	910.54	568.89
T (K)	120(2)	120(2)
λ (Å)	0.71070	0.71070
Crystal system	Monoclinic	Monoclinic
Space group	$P2_1/n$	$P2_1/c$
a (Å)	12.883(5)	14.453(11)
b (Å)	10.344(4)	10.260(8)
c (Å)	16.539(7)	15.554(12)
α (°)	90	90
β (°)	111.7413(14)	95.144(4)
γ (°)	90	90
V (Å^3)	2047.3(14)	2297(3)
Z	2	4
D_{calc} (g/cm^3)	1.477	1.645
μ (mm^{-1})	1.115	1.015
F(000)	936	1160
Crystal size (mm)	0.40 × 0.40 × 0.05	0.50 × 0.40 × 0.10
2θ range (°)	3.19–24.99	3.10–25.00
Reflections collected	12794	14296
Independent reflections/R_{int}	3586/0.0305	3997/0.1102
Parameters	224	291
GOF on F^2	1.143	0.982
R_1, wR_2 [$I > 2\sigma(I)$]	0.0381, 0.0779	0.0521, 0.1222
R_1, wR_2 (all data)	0.0436, 0.0826	0.0632, 0.1422

The value of electron density $\rho(\mathbf{r}) = 0.01778$ in **8** at BCP between Pd(1)–C(17) indicates the strengths of the interactions are similar to the previously reported intramolecular C–H agnostic interactions between arene C–H bond and cadmium in cadmium(II)-benziporphyrin complexes ($\rho(\mathbf{r}) = 0.0186$) [56] or between C–H bond of ^{t}Bu group and palladium in (^{t}Bu$_3$P)PdPhX (X = Br, I) complexes ($\rho(\mathbf{r}) = 0.018$, 0.017) [54]. Recently, Barder reported an application of QTAIM analysis for estimation of stronger η^1-coordinations in **11** ($\rho(\mathbf{r}) = 0.0740$, 0.0618) [57]. The values of electron density, $\rho(\mathbf{r}) = 0.03822$ for Pd(1)–C(16), 0.03994 for Pd(1)–C(17) at BCP in **9**, indicate the relatively stronger η^2-coordination in **9** than η^1-coordination in **8**. However, this η^2-coordination in **9** is still weaker than the usual σ-coordination from phosphorus, carbon, or chlorine atoms to the central palladium as we can see in Table 3.

All the values of $\nabla^2\rho(\mathbf{r})$ are positive, indicating all the interactions have an ionic character even in the weakest interaction between Pd(1) and C(17) in **8**. As described in Fig. 4, the bond path between Pd(1) and C(17) in **8** is perpendicular to C(16)–C(17) bond to show that the interaction is a weak η^1-coordination but not C–H agostic interaction. Shapes of bond paths among Pd(1), C(16), and C(17) in **9** reflect a simultaneous coordination of two carbon atoms, that is η^2-coordination.

3. Conclusion

Two new methylpalladium complexes Pd(**1**)(Me)Cl (**8**) and Pd(**1**)(Me)OTf (**9**) were synthesized and structurally characterized. X-ray diffraction revealed that **8** had a chloride-bridged dinuclear structure with a possibility for the existence of a weak η^1-interaction from *ortho* carbon of the terminal phenyl ring as a fifth coordination. In contrast, **9** showed a η^2-coordination of the phenyl ring of the biphenyl moiety although the NMR study revealed the η^2-coordination is very weak. The structural difference in these complexes may come from the electron density of the central palladium atom and the bridging ability of the anionic ligand. These weak interactions were also suggested to exist by NBO and QTAIM calculation.

4. Experimental

4.1. General

All manipulations were carried out using standard Schlenk techniques or in the glove box under argon atmosphere. All NMR spectra were recorded using JEOL ECP500 spectrometer. $CHCl_3$ (^1H), $CDCl_3$ (^{13}C), and 85% H_3PO_4 (^{31}P) were employed as internal and external standards. Mass spectra was recorded on a JEOL JMS-AX505H spectrometer using PEG calibration. Melting points were measured on a Yanagimoto micro melting point apparatus MP-500D and are uncorrected. ^{t}Bu$_2$P(biphenyl-2-yl) and AgOTf were purchased and were used without further purification. Solvents were purified by solvent purification system of Glass-Contour. (cod)Pd(Me)Cl[36] was prepared according to the literature.

4.2. Synthesis of {[^{t}Bu$_2$P(biphenyl-2-yl)]Pd(Me)Cl}$_2$ (8)

To a mixture of ^{t}Bu$_2$P(biphenyl-2-yl) (1.98 g, 6.60 mmol) and (cod)Pd(Me)Cl (1.67 g, 6.30 mmol), CH_2Cl_2 (7 mL) was added at room temperature. The reaction mixture was stirred at room temperature for 19 h, and was poured into a vigorously stirred hexane to precipitate a dark-yellow solid. The resulting solid was isolated by filtration through a filtering paper to give the desired product (2.59 g, 90%). ^1H NMR ($CDCl_3$, 500 MHz) δ 1.47 (d, $J = 14$ Hz, 18H), 1.55 (d, $J = 2$ Hz, 3H), 6.80–6.83 (m, 1H), 7.15 (d, $J = 7.5$ Hz, 2H), 7.36–7.40 (m, 2H), 7.50 (t, $J = 7.8$ Hz, 2H), 7.75 (t, $J = 7.5$ Hz, 1H), 7.92–7.95 (m, 1H); $^{13}C\{^1H\}$ NMR ($CDCl_3$, 125 MHz) δ −0.71 (CH_3), 31.3 (d, $J = 4.8$ Hz, CH_3), 38.5 (d, $J = 16$ Hz, 4°), 126.1 (d, $J = 4.8$ Hz, CH), 126.2 (CH), 130.4 (CH), 131.0 (d, $J = 31$ Hz, 4°), 131.4 (CH), 131.9 (CH), 133.2 (d, $J = 9.5$ Hz, CH), 133.6 (d, $J = 5.0$ Hz, 4°), 134.5 (CH), 149.2 (d, $J = 19$ Hz, 4°); $^{31}P\{^1H\}$ NMR ($CDCl_3$, 202 MHz) δ 62.4 (s); m.p. 136.4–137.4 °C (dec.). Anal. Calc. for $C_{21}H_{30}ClPPd$: C, 55.40; H, 6.64. Found: C, 55.15; H, 6.77%.

4.3. Synthesis of [^{t}Bu$_2$P(biphenyl-2-yl)]Pd(Me)OTf (9)

To a mixture of AgOTf (0.526 g, 2.05 mmol) and **1** (0.456 g, 1.00 mmol), CH_2Cl_2 (7 mL) was added at room temperature. The reaction mixture was stirred at room temperature for 10 min. The resulting solution was filtered through a Celite pad, and was poured into a vigorously stirred hexane to precipitate a pale-yellow solid. The resulting solid was washed with hexane three times to give the desired product (0.415 g, 71%). ^1H NMR ($CDCl_3$, 500 MHz) δ 1.48 (d, $J = 15$ Hz, 18H), 1.54 (s, 3H), 6.86–6.92 (m, 1H), 7.27 (d, $J = 7.3$ Hz, 2H), 7.41–7.46 (m, 2H), 7.63 (t, $J = 7.5$ Hz, 2H), 7.70 (t, $J = 7.5$ Hz, 1H), 7.90–7.95 (m, 1H); $^{13}C\{^1H\}$ NMR ($CDCl_3$, 125 MHz) δ 5.01 (CH_3), 31.2 (d, $J = 3.8$ Hz, CH_3), 39.1 (d, $J = 17.5$ Hz, 4°), 119.6 (d, $^1J_{CF} = 318$ Hz, CF_3), 125.5 (CH), 126.4 (d, $J = 4.8$ Hz, CH), 129.7 (d, $J = 36.3$ Hz, 4°), 131.0 (CH), 131.6 (CH), 132.3 (d, $J = 3.8$ Hz, 4°), 132.9 (d, $J = 9.5$ Hz, CH), 133.5 (CH), 133.9 (CH), 148.6 (d, $J = 15.3$ Hz); $^{31}P\{^1H\}$ NMR ($CDCl_3$, 202 MHz) δ 71.6 (s); $^{19}F\{^1H\}$ NMR ($CDCl_3$, 470 MHz) $\delta - 77.6$ (s); m.p. 136.4–137.4 °C (dec.); HRMS–FAB (*m/z*): $[M - CF_3SO_3]^+$ Calc. for $C_{21}H_{30}PPd$, 417.1126, 418.1136, 419.1120, 421.1124, 423.1137. Found: 417.1082, 418.1123, 419.1123, 421.1117, 423.1122%.

4.4. X-ray crystallography

Details of the crystal data and a summary of the intensity data collection parameters for **8** and **9** are listed in Table 2. Crystal data were deposited to Cambridge Crystallographic Data Centre as CCDC – 295496 and 295497. In each case a suitable crystal was mounted with a mineral oil to the glass fiber and transferred to the goniometer of a Rigaku Mercury CCD diffractometer with graphite-monochromated Mo Kα radiation ($\lambda = 0.71069$ Å) to $2\theta_{max} = 55°$. The structures were solved by direct methods with (SIR-97 [59] or SHELXS [60]) and refined by full-matrix least-squares techniques against F^2 (SHELXL-97 [60]). The intensities were corrected for Lorentz and polarization effects. The non-hydrogen atoms were refined anisotropically. Hydrogen atoms were refined isotropically in the difference Fourier maps or placed using AFIX instructions.

Acknowledgments

We thank Prof. Takayuki Kawashima and Prof. Kei Goto at Graduate School of Science, the University of Tokyo for use of X-ray diffractometer. M.Y. thanks Dr. Takahiro Sasamori at the Institute for Chemical Research, Kyoto University for helpful discussions.

Appendix A. Supplementary data

CIF files of **8** and **9**. Supplementary data associated with this article can be found, in the online version, at doi:10.1016/j.jorganchem.2006.02.001.

References

[1] D.W. Old, J.P. Wolfe, S.L. Buchwald, J. Am. Chem. Soc. 120 (1998) 9722–9723.
[2] B.H. Yang, S.L. Buchwald, J. Organomet. Chem. 576 (1999) 125–146.
[3] J.P. Wolfe, S.L. Buchwald, Angew. Chem. Int. Ed. 38 (1999) 2413–2416.
[4] A.R. Muci, S.L. Buchwald, Top. Curr. Chem. 219 (2001) 131–209.
[5] K.E. Torraca, X.H. Huang, C.A. Parrish, S.L. Buchwald, J. Am. Chem. Soc. 123 (2001) 10770–10771.
[6] S. Kuwabe, K.E. Torraca, S.L. Buchwald, J. Am. Chem. Soc. 123 (2001) 12202–12206.
[7] J. Yin, M.P. Rainka, X.-X. Zhang, S.L. Buchwald, J. Am. Chem. Soc. 124 (2002) 1162–1163.
[8] E.R. Strieter, D.G. Blackmond, S.L. Buchwald, J. Am. Chem. Soc. 125 (2003) 13978–13980.
[9] H.N. Nguyen, X. Huang, S.L. Buchwald, J. Am. Chem. Soc. 125 (2003) 11818–11819.
[10] X. Huang, K.W. Anderson, D. Zim, L. Jiang, A. Klapars, S.L. Buchwald, J. Am. Chem. Soc. 125 (2003) 6653–6655.
[11] T.E. Barder, S.L. Buchwald, Org. Lett. 6 (2004) 2649–2652.
[12] J.E. Milne, S.L. Buchwald, J. Am. Chem. Soc. 126 (2004) 13028–13032.
[13] S.D. Walker, T.E. Barder, J.R. Martinelli, S.L. Buchwald, Angew. Chem. Int. Ed. 43 (2004) 1871–1876.
[14] K.W. Anderson, S.L. Buchwald, Angew. Chem. Int. Ed. 44 (2005) 6173–6177.
[15] M.D. Charles, P. Schultz, S.L. Buchwald, Org. Lett. 7 (2005) 3965–3968.
[16] A.V. Vorogushin, X.H. Huang, S.L. Buchwald, J. Am. Chem. Soc. 127 (2005) 8146–8149.
[17] T.E. Barder, S.D. Walker, J.R. Martinelli, S.L. Buchwald, J. Am. Chem. Soc. 127 (2005) 4685–4696.
[18] Y. Uozumi, T. Hayashi, J. Am. Chem. Soc. 113 (1991) 9887–9888.
[19] Y. Uozumi, A. Tanahashi, S.Y. Lee, T. Hayashi, J. Org. Chem. 58 (1993) 1945–1948.
[20] T. Hayashi, H. Iwamura, M. Naito, Y. Matsumoto, Y. Uozumi, M. Miki, K. Yanagi, J. Am. Chem. Soc. 116 (1994) 775–776.
[21] Y. Uozumi, K. Kitayama, T. Hayashi, K. Yanagi, E. Fukuyo, Bull. Chem. Soc. Jpn. 68 (1995) 713–722.
[22] T. Hayashi, J. Organomet. Chem. 576 (1999) 195–202.
[23] T. Hayashi, Acc. Chem. Res. 33 (2000) 354–362.
[24] Y. Kawashima, K. Okano, K. Nozaki, T. Hiyama, Bull. Chem. Soc. Jpn. 77 (2004) 347–355.
[25] S. Vyskocil, M. Smrcina, V. Hanus, M. Polasek, P. Kocovsky, J. Org. Chem. 63 (1998) 7738–7748.
[26] K.L. Ding, Y. Wang, H.Y. Yun, J.X. Liu, Y.J. Wu, M. Terada, Y. Okubo, K. Mikami, Chem. Eur. J. 5 (1999) 1734–1737.
[27] P. Kocovsky, S. Vyskocil, I. Cisarova, J. Sejbal, I. Tislerova, M. Smrcina, G.C. Lloyd-Jones, S.C. Stephen, C.P. Butts, M. Murray, V. Langer, J. Am. Chem. Soc. 121 (1999) 7714–7715.
[28] P. Dotta, P.G.A. Kumar, P.S. Pregosin, A. Albinati, S. Rizzato, Organometallics 22 (2003) 5345–5349.
[29] Y. Wang, X. Li, J. Sun, K.L. Ding, Organometallics 22 (2003) 1856–1862.
[30] J.W. Faller, N. Sarantopoulos, Organometallics 23 (2004) 2008–2014.
[31] P. Dotta, P.G.A. Kumar, P.S. Pregosin, A. Albinati, S. Rizzato, Organometallics 23 (2004) 4247–4254.
[32] S.M. Reid, R.C. Boyle, J.T. Mague, M.J. Fink, J. Am. Chem. Soc. 125 (2003) 7816–7817.
[33] P. Dotta, P.G.A. Kumar, P.S. Pregosin, A. Albinati, Helv. Chim. Acta 87 (2004) 272–278.
[34] U. Christmann, R. Vilar, A.J.P. White, D. Williams, J. Chem. Commun. (2004) 1294–1295.
[35] P.G.A. Kumar, P. Dotta, R. Hermatschweiler, P.S. Pregosin, A. Albinati, S. Rizzato, Organometallics 24 (2005) 1306–1314.
[36] R.E. Rulke, J.M. Ernsting, A.L. Spek, C.J. Elsevier, P.W.N.M. Vanleeuwen, K. Vrieze, Inorg. Chem. 32 (1993) 5769–5778.
[37] F.T. Ladipo, G.K. Anderson, Organometallics 13 (1994) 303–306.
[38] A. Aranyos, D.W. Old, A. Kiyomori, J.P. Wolfe, J.P. Sadighi, S.L. Buchwald, J. Am. Chem. Soc. 121 (1999) 4369–4378.
[39] J.P. Wolfe, R.A. Singer, B.H. Yang, S.L. Buchwald, J. Am. Chem. Soc. 121 (1999) 9550–9561.
[40] In Ref. [36], the authors claimed that **1** showed 15 aromatic peaks in $CDCl_3$ solution without complete assignment due to complex P–C coupling. However, our observation of ^{13}C NMR spectra of **1** showed 10 kinds of aromatic signals containing 4 doublets split by P–C coupling. This result indicates that the phenyl ring is freely rotating in the NMR time scale. ^{13}C NMR of **1** ($CDCl_3$, 125 MHz) δ 30.9 (d, $J = 15.3$ Hz, $C(CH_3)_3$), 32.9 (d, $J = 24.8$ Hz, $C(CH_3)_3$), 125.9 (CH), 126.5 (CH), 127.2 (CH), 128.5 (CH), 130.69 (CH), 130.72 (CH), 135.5 (d, $J = 2.9$ Hz, CH), 135.7 (d, $J = 27.8$ Hz, 4°), 143.9 (d, $J = 7.7$ Hz, 4°), 151.4 (d, 32.6 Hz, 4°).
[41] J.D. Oliver, D.F. Mullica, W.O. Milligan, Inorg. Chem. 21 (1982) 3284–3286.
[42] W.J. Youngs, J. Mahood, B.L. Simms, P.N. Swepston, J.A. Ibers, M.Y. Shang, J.L. Huang, J.X. Lu, Organometallics 2 (1983) 917–921.
[43] S.J. Geib, A.L. Rheingold, Acta Crystallogr., Sect. C 43 (1987) 1427–1428.
[44] E.C. Alyea, G. Ferguson, J. Malito, B.L. Ruhl, Organometallics 8 (1989) 1188–1191.
[45] F. Paul, P. Joe, J.F. Hartwig, Organometallics 14 (1995) 3030–3039.
[46] B.J. Burke, L.E. Overman, J. Am. Chem. Soc. 126 (2004) 16820–16833.
[47] A. Bondi, J. Phys. Chem. 68 (1964) 441–451.
[48] K.B. Wiberg, Tetrahedron 24 (1968) 1083–1096.
[49] R.F.W. Bader, Atoms in Molecules – A Quantum Theory, Oxford University Press, New York, 1990.
[50] R.F.W. Bader, Chem. Rev. 91 (1991) 893–928.
[51] M.J. Frisch, G.W. Trucks, H.B. Schlegel, G.E. Scuseria, M.A. Robb, J.R. Cheeseman, J.A. Montgomery, T. Vreven, K.N. Kudin, J.C. Burant, J.M. Millam, S.S. Iyengar, J. Tomasi, V. Barone, B. Mennucci, M. Cossi, G. Scalmani, N. Rega, G.A. Petersson, H. Nakatsuji, M. Hada, M. Ehara, K. Toyota, R. Fukuda, J. Hasegawa, M. Ishida, T. Nakajima, Y. Honda, O. Kitao, H. Nakai, M. Klene, X. Li, J.E. Knox, H.P. Hratchian, J.B. Cross, V. Bakken, C. Adamo, J. Jaramillo, R. Gomperts, R.E. Stratmann, O. Yazyev, A.J. Austin, R. Cammi, C. Pomelli, J.W. Ochterski, P.Y. Ayala, K. Morokuma, G.A. Voth, P. Salvador, J.J. Dannenberg, V.G. Zakrzewski, S. Dapprich, A.D. Daniels, M.C. Strain, O. Farkas, D.K. Malick, A.D. Rabuck, K. Raghavachari, J.B. Foresman, J.V. Ortiz, Q. Cui, A.G. Baboul, S. Clifford, J. Cioslowski, B.B. Stefanov, G. Liu, A. Liashenko, P. Piskorz, I. Komaromi, R.L. Martin, D.J. Fox, T. Keith, Al.-M.A. Laham, C.Y. Peng, A. Nanayakkara, M. Challacombe, P.M.W. Gill, B. Johnson, W. Chen, M.W. Wong, C. Gonzalez, J.A. Pople, GAUSSIAN03w, Revision B.03, Gaussian, Inc., Wallingford, CT, 2004.
[52] F. Biegler-Konig, J. Schonbohm, D. Bayles, J. Comput. Chem. 22 (2001) 545–559.
[53] F. Biegler-Konig, J. Schonbohm, J. Comput. Chem. 23 (2002) 1489–1494.
[54] J.P. Stambuli, C.D. Incarvito, M. Buhl, J.F. Hartwig, J. Am. Chem. Soc. 126 (2004) 1184–1194.
[55] M. Niemeyer, Z. Anorg. Allg. Chem. 628 (2002) 647–657.
[56] M. Stepien, L. Latos-Grazynski, L. Szterenberg, J. Panek, Z. Latajka, J. Am. Chem. Soc. 126 (2004) 4566–4580.

[57] T.E. Barder, J. Am. Chem. Soc. 128 (2006) 898–904.

[58] Less significant relationship between WBI and $\rho(\mathbf{r})$ is in contrast to the case of that the positive correlation between WBI and $\rho(\mathbf{r})$ was observed in hydrogen bonding of water with acetic acid. V.S. Znamenskiy, M.E. Green, J. Phys. Chem. A 108 (2004) 6543–6553.

[59] A. Altomare, M.C. Burla, M. Camalli, G.L. Cascarano, C. Giacovazzo, A. Guagliardi, A.G.G. Moliterni, G. Polidori, R. Spagna, J. Appl. Crystallogr. 32 (1999) 115–119.

[60] G.M. Sheldrick, SHELXL-97, Program for the Refinement of Crystal Structures, University of Göttingen, Göttingen, Germany, 1997.